Supplmentary Material for - The Generic Time Clustering of Low Frequency Earthquakes and Intermittent Creep

O. Lengliné[a], W. B. Frank[b], D. Marsan[c], J.-P. Ampuero[d]

[a] *Université de Strasbourg, EOST, IPGS, CNRS, Strasbourg, France*
[b] *Department of Earth, Athmospheric, and Planetary Sciences, MIT, Cambridge, USA*
[c] *Université de Savoie, IsTerre, CNRS, Le Bourget du Lac, France*
[d] *Seismolab, Caltech, Pasadena, USA*

This file contains all the supplementary information for The Generic Time Clustering of Low Frequency Earthquakes and Intermittent Creep. It includes Figures S1-S7 and the Supplementary Discussions about: comparison of the kernel g with LFE recurrence times and, the selection of burst onset times.

Normalized reccurence times

To estimate if the behaviors revealed by the triggering kernels represent a real feature of the LFE activity, we employ a different, model-independent approach to constrain the time clustering of LFEs at short time scales. We first compute the recurrence times, Δt, which we define as the time interval between two successive LFEs. We then normalize these recurrence times by the mean recurrence time of the family, $\langle \Delta t \rangle$ in order to obtain $\overline{\Delta t} = \Delta t / \langle \Delta t \rangle$. We use the normalized recurrence times of LFEs within each family to obtain the probability density function (pdf), f, of $\overline{\Delta t}$. We observe at short time scales a power-law decay of the pdf, $f(\overline{\Delta t}) \sim \overline{\Delta t}^{-q}$, with a power law exponent of q. This behavior is common to all families in this catalog (Figure S1). We compute the power-law exponent, q, of the decay of the pdf at short time-scales over the normalized time interval $\overline{\Delta t} \in [10^{-3} - 1]$. This leads to a mean value of q of 1.0 (Figure S1).

We applied the same processing to the LFE catalogs in the Cascadia subduction and Parkfield. We find that the normalized inter-event time distributions for each family in this area follow a power-law decay over most of the range (Figure S1), with mean q value of 1.33. In contrast, in the Parkfield area we find that the behavior of $f(\overline{\Delta t})$ differs from one family to another (Figure S1). For some families, we find a single power law decay of the normalized recurrence times pdf (Figure S1), while other families present a second power law decay starting at longer time scales. This varied behavior among LFE families in Parkfield was previously recognized [*Shelly 2010, Wuet al., 2015*]. The power law trend decay considering only intervals $10^{-4} < \overline{\Delta t} < 10^{-2}$ has a mean q value of 1.88.

Selection of burst onset times

We illustrate with Figure S4 how do we operate the burst selection based on the criterion ω_0 and a. We also show in Figure S5 the influence of the treshold values, a_c and w_{0c} on the behavior of the functions C_+ describing the LFE burst shape. We notably observe that changing the values

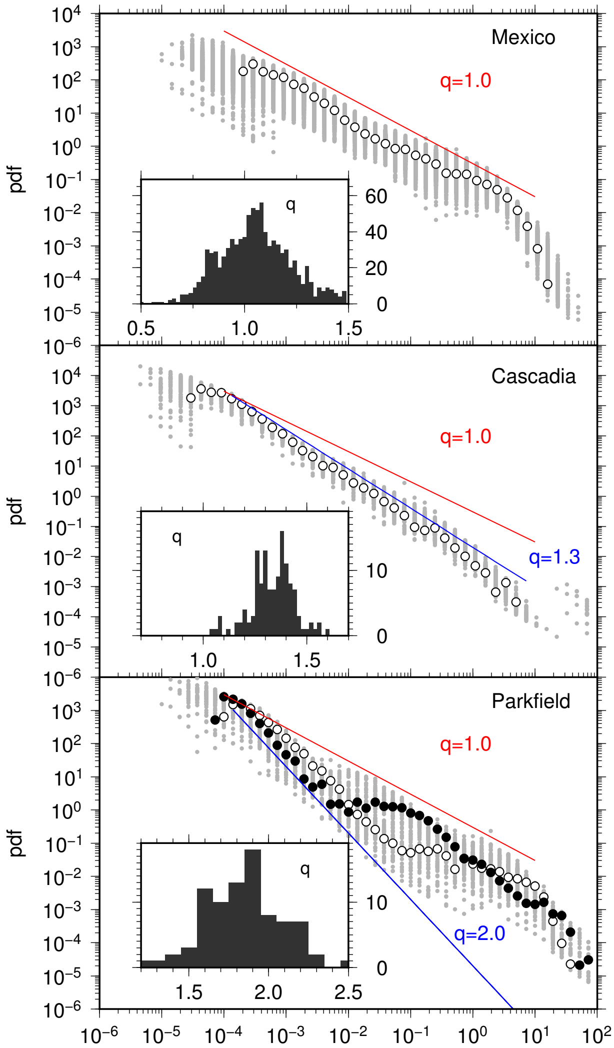

Figure S1: Probability density functions of the normalized inter-event times, $f(\overline{\Delta t})$, for all families (gray points) and for one example family (white circles) which is the same family as in Figure **??**). The red and blue curves show power-law decays with different exponents for reference. The histogram represents the values of the power law exponent q obtained for all families (black rectangles). For the Parkfield catalog, two families (black and white circles) are shown which are representative of the two different behaviors we observe.

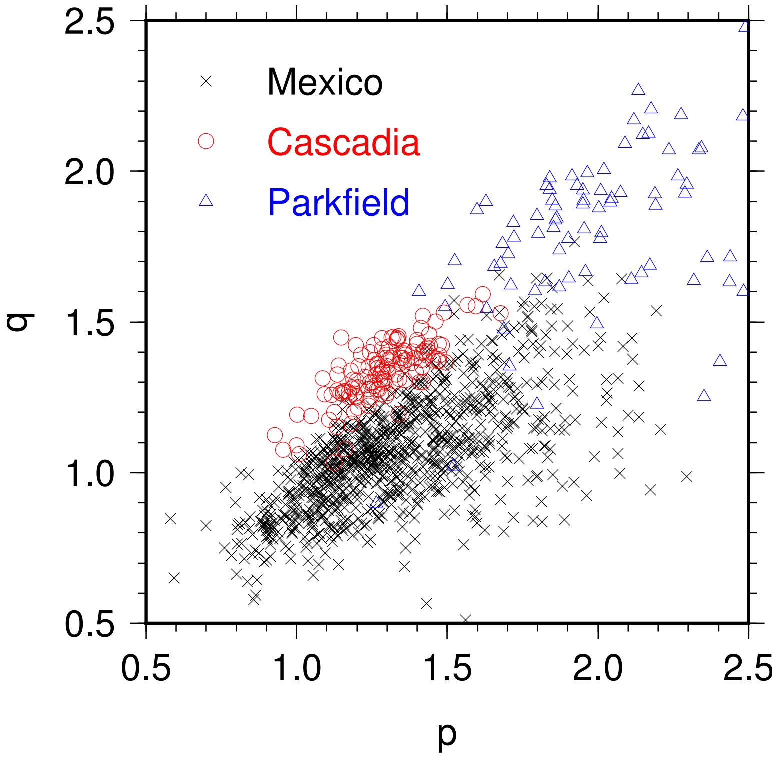

Figure S2: Comparison between the value of q and p for the three catalogs and for each family. We observa correlation between the two parameters for each catalog. One should note however that the two distributions are not exactly equal since q quantifies the decay rate of the inter-event time while p is the power-law exponent of the LFE rate.

of the threshold do not significantly affect the shape of the recovered curves. It highlights that our burst definition appears stable relative to the parameters entering its definition.

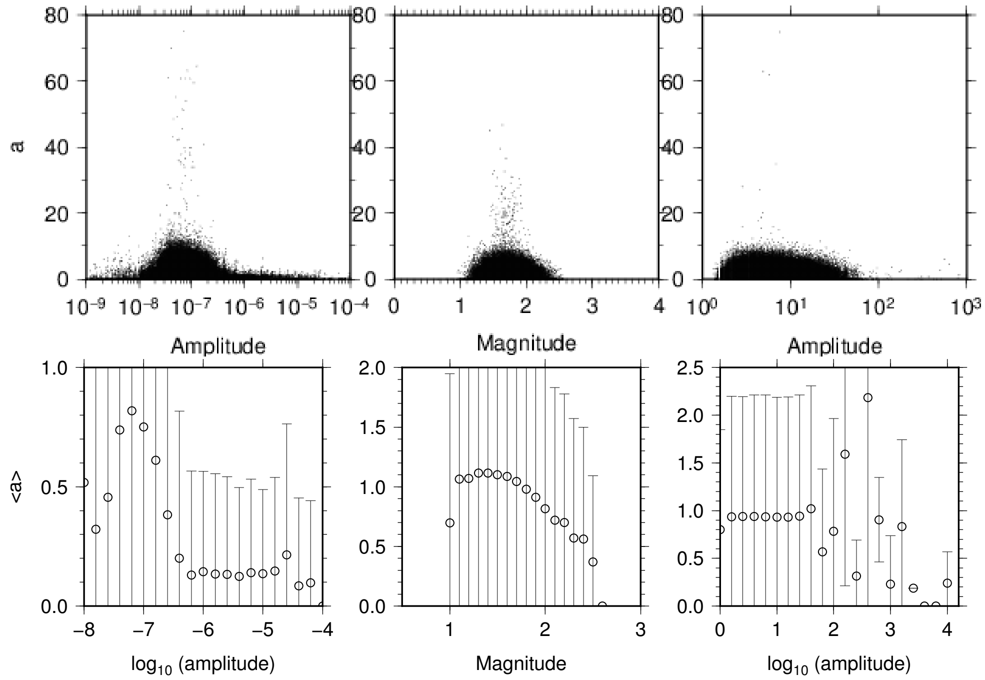

Figure S3: Top: The black dots represent for each LFE their waveform amplitude (on logarithmic scale) or magnitude as reported in the catalog as a function of the parameter *a* representing the triggering amplitude obtained from the Expectation-Maximization algorithm. Bottom: same as above but for each amplitude/magnitude interval we compute the average value of *a* (circles) and its standard deviation (error bars).

Testing the best recurrence times

Following *Wu et al., 2015*, we consider burst episodes for a given family when at least 10 events occurred in a time interval less than $4\langle\Delta t\rangle$. After the identification of the burst occurrence times we proceed as described in the main manuscript to obtain normalized inter-burst times. We use this approach on the Mexican and Parkfield catalogs because burst identification for the Cascadia catalog is straightforward given that LFEs are only detected during reported SSEs. We observe for both Mexico and Parkfield catalogs a distribution of recurrence times compatible with the distributions obtained previously (Fig. S6). We test for both these catalogs that changing the required number of LFEs to less than $4\langle\Delta t\rangle$ from 5 to 20 does not affect the distribution and still captures the burst episodes. These results confirmed those obtained previously and show that the recurrence times over the interface are well approximated by a log-normal distribution.

References

Wu, C., Guyer, R., Shelly, D., Trugman, D., Frank, W., Gomberg, J., and Johnson, P. (2015). Spatial-temporal variation of low-frequency earthquake bursts near Parkfield, California. Geophysical Journal International, 202(2), 914-919.

Shelly, D. R. (2010). Periodic, chaotic, and doubled earthquake recurrence intervals on the deep San Andreas Fault. Science, 328(5984), 1385-1388.

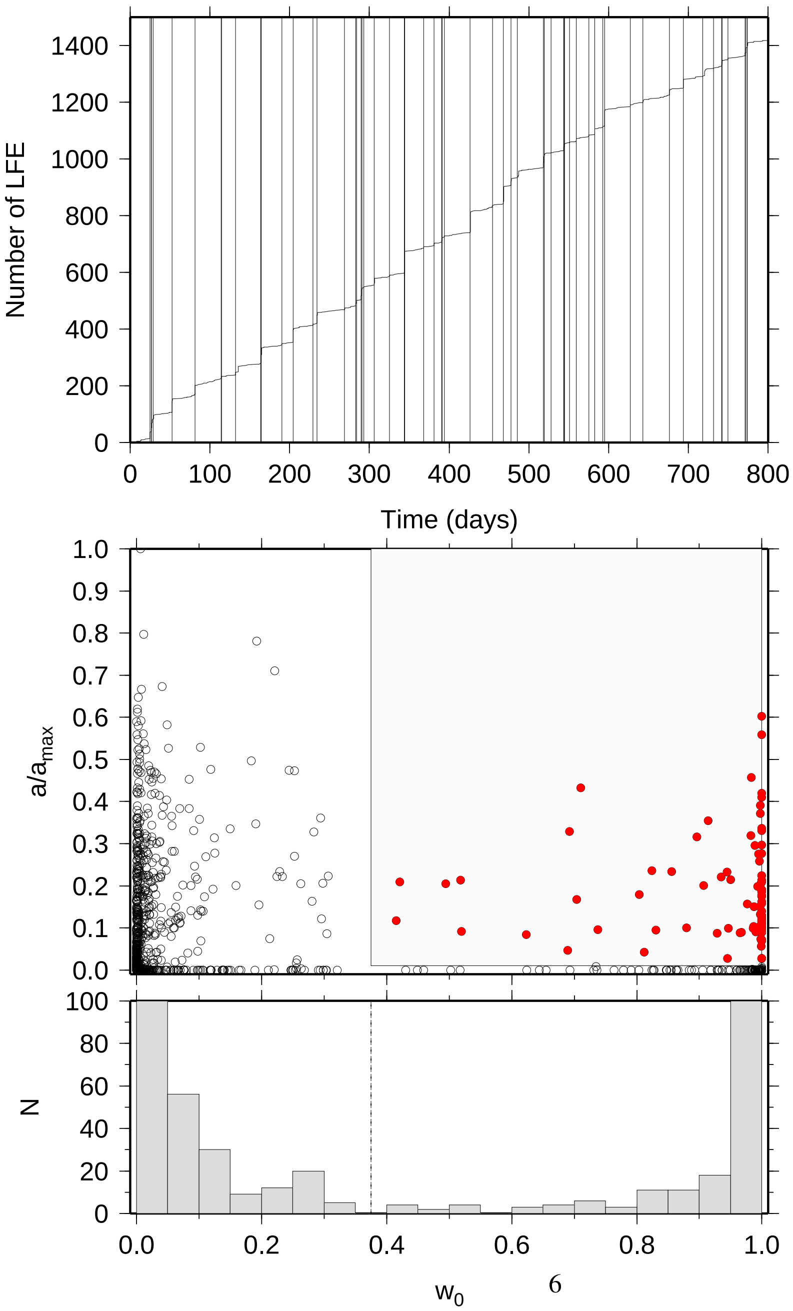

Figure S4: Example of the burst onset selection for the family 301 of the Mexican catalog. Top: Cumulative numebr of LFE as a function of time in this family. The vertical dark lines mark the identified burst onsets. Middle: Each circle represents an LFE and its associated values of w_0 and a/a_{max}, where a_{max} is the maximum value of a for this family. The gray area represents the values of w_0 and a above the fixed thresholds and thus considered as burs onset (red circles). Here a_c is fixed at 0.1 and w_{0c} is given by the position of the minimum of the distribution of w_0. Bottom : Distribution of w_0 value for the family 301. The vertical line indicates the location of the minimum of this distribution and thus defines the threshold w_{0c}. Note that for the first and the last interval the graph saturates.

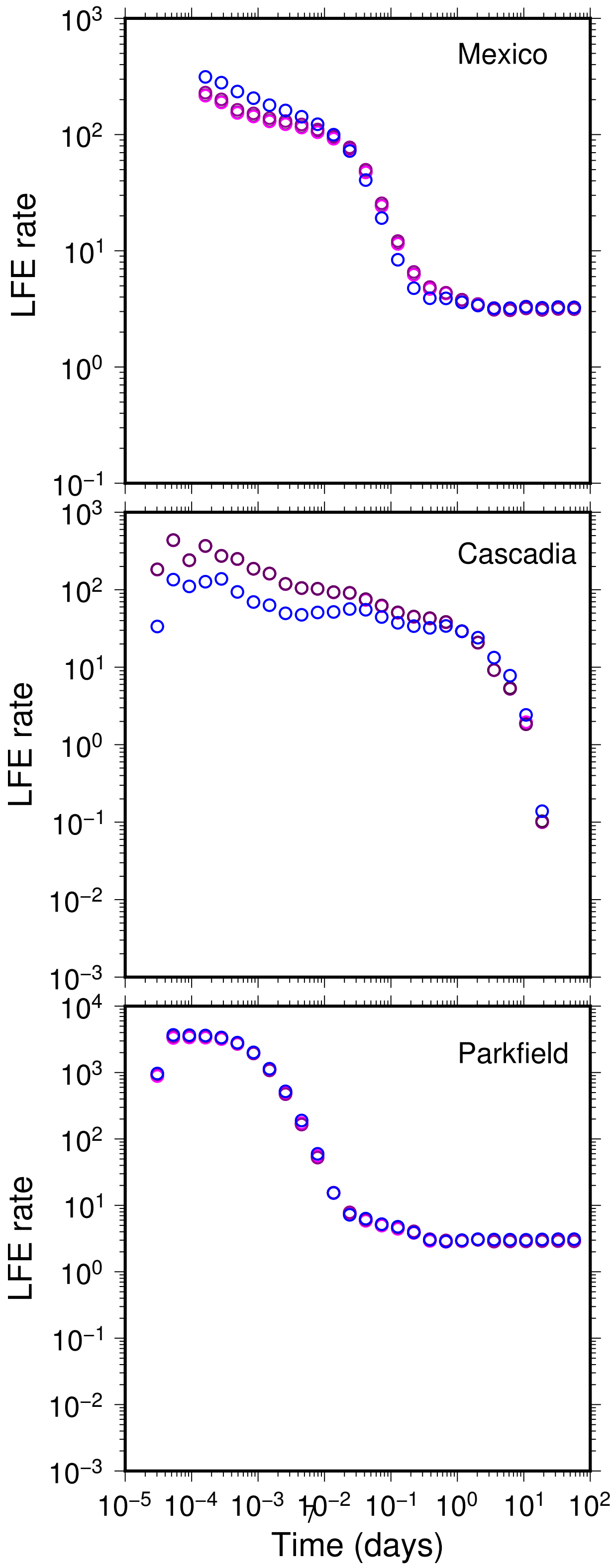

Figure S5: Influence of the selection thresholds for the burst definition on the shape of the function C. For each catalog we vary either the value of a_c or the value of w_{0c}. The black circles represents the selection used in the manuscript, the pink/purples circles correspond to changing a_c to $1 \cdot 10^{-2}$ / $5 \cdot 10^{-2}$ and the blue circles to using a fixed value of w_{0c} here fixed at 0.1 for all families.

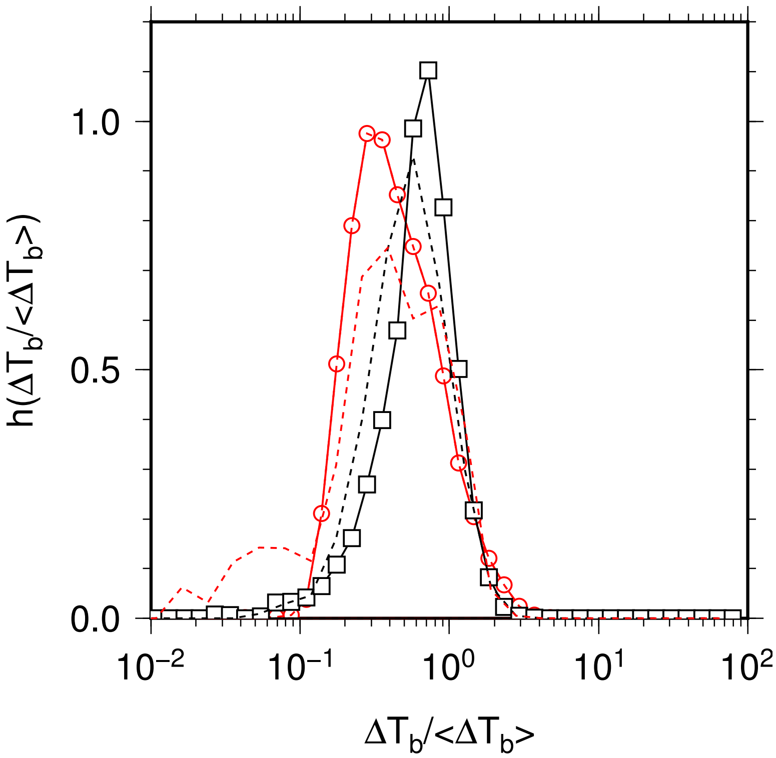

Figure S6: Same figure as figure 7 in the main text representing the normalized burst inter-event times. In this figure, burst times have been computed following the approach presented in *Wu et al. 2015..* .

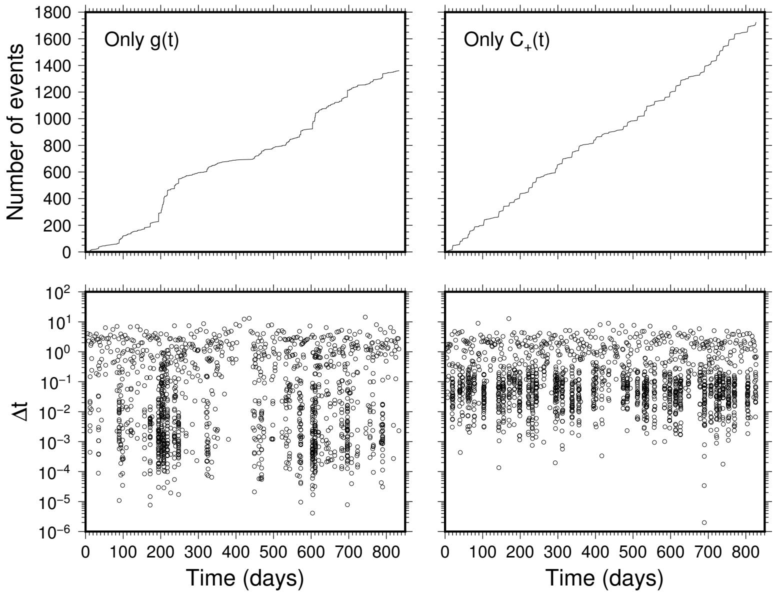

Figure S7: Example of random realizations of a generated LFE family. This reealization was generated based on statistical properties of the family reported in Figure 1 in the manuscript. Top: cumulative number of LFEs in the family as a function of time. Middle: Recurrence time of LFE as a function of time. The figures on the left represent the first scenario where LFE are generated following the function g without considering the LFE burst behavior. The figures on the right represent the scenario where LFE are simply generated by the function C_+. We observe in this last case that we lack short time clustering of the LFE activity as visible in the recurrence times.